

# Evaluation of a new neutron energy spectrum unfolding code based on an Adaptive Neuro-Fuzzy Inference System (ANFIS)

Seyed Abolfazl Hosseini<sup>1,\*</sup> and Iman Esmaili Paen Afrakoti<sup>2</sup>

<sup>1</sup>Department of Energy Engineering, Sharif University of Technology, Tehran, 8639–11365, Iran

<sup>2</sup>Faculty of Engineering & Technology, University of Mazandaran, PO Box: 416, Pasdaran Street, Babolsar, 47415, Iran

\*Corresponding author. Department of Energy Engineering, Sharif University of Technology, Tehran, 8639–11365, Iran.

Tel: +98 21 6616 6140; Fax: +98 21 66081723; Email: sahosseini@sharif.edu

(Received 20 May 2017; revised 9 October 2017; editorial decision 8 December 2017)

## ABSTRACT

The purpose of the present study was to reconstruct the energy spectrum of a poly-energetic neutron source using an algorithm developed based on an Adaptive Neuro-Fuzzy Inference System (ANFIS). ANFIS is a kind of artificial neural network based on the Takagi–Sugeno fuzzy inference system. The ANFIS algorithm uses the advantages of both fuzzy inference systems and artificial neural networks to improve the effectiveness of algorithms in various applications such as modeling, control and classification. The neutron pulse height distributions used as input data in the training procedure for the ANFIS algorithm were obtained from the simulations performed by MCNPX-ESUT computational code (MCNPX-Energy engineering of Sharif University of Technology). Taking into account the normalization condition of each energy spectrum, 4300 neutron energy spectra were generated randomly. (The value in each bin was generated randomly, and finally a normalization of each generated energy spectrum was performed). The randomly generated neutron energy spectra were considered as output data of the developed ANFIS computational code in the training step. To calculate the neutron energy spectrum using conventional methods, an inverse problem with an approximately singular response matrix (with the determinant of the matrix close to zero) should be solved. The solution of the inverse problem using the conventional methods unfold neutron energy spectrum with low accuracy. Application of the iterative algorithms in the solution of such a problem, or utilizing the intelligent algorithms (in which there is no need to solve the problem), is usually preferred for unfolding of the energy spectrum. Therefore, the main reason for development of intelligent algorithms like ANFIS for unfolding of neutron energy spectra is to avoid solving the inverse problem. In the present study, the unfolded neutron energy spectra of <sup>252</sup>Cf and <sup>241</sup>Am-<sup>9</sup>Be neutron sources using the developed computational code were found to have excellent agreement with the reference data. Also, the unfolded energy spectra of the neutron sources as obtained using ANFIS were more accurate than the results reported from calculations performed using artificial neural networks in previously published papers.

**Keywords:** neutron energy spectrum; unfolding; neutron pulse height distribution; ANFIS; <sup>241</sup>Am-<sup>9</sup>Be; <sup>252</sup>Cf

## INTRODUCTION

Accurate knowledge of neutron energy spectra has significant usage in much basic research and in many applications such as in nuclear non-proliferation, international safeguarding, nuclear material control, national security and counterterrorism [1]. The accurate unfolding of neutron spectra increases the sensitivity of assays performed on various nuclear materials [2]. The use of interrogation and

reconstruction techniques for detection of special nuclear materials and neutron sources via energy spectra has been widely investigated [3].

To unfold a neutron energy spectrum with a high degree of accuracy, the appropriate detector should be selected for accurate simulation of the neutron pulse height distribution. NE-213 liquid scintillation detectors are widely used for fast neutron spectroscopy because of

their good linearity, excellent neutron–gamma discrimination property and high light output [4]. Several studies have been performed in recent years to evaluate the performance of some specialized computational codes for simulation of the neutron pulse height distribution. A full review of papers published about the simulation of neutron pulse height distribution has been presented in the paper published by Hosseini and his colleagues [5]. The main motivation for the present work was development of a computational code, based on the neuro fuzzy algorithm for energy spectra unfolding of neutron sources, that would have a low calculation cost (i.e. a high degree of accuracy, yet a low execution time). To this end, the required neutron pulse height distribution was calculated using the developed MCNPX-ESUT computational code [5]. To unfold the energy spectrum of a neutron source via solution of the inverse problem using conventional methods, the neutron response matrix that links the neutron energy spectrum with the pulse height distribution should be known. The inverse problem of determining the radiation source information from simulated/measured detector readings has been investigated by many researchers. Modern unfolding code packages that employ these techniques include MAXED [6], UNFANA [7], HEPRO [8] and FORIST [9]. Other methods, such as using an artificial neural network [3, 10], may be used for the unfolding of neutron energy spectra. The unfolded neutron energy spectrum obtained using an artificial neural network has acceptable accuracy [10]; however, the calculation cost reported in the cited papers is relatively high. The aim of the present work was to develop a computational code that gives highly accurate results with low calculation costs. To this end, in the present paper, neutron energy spectra of neutron sources were reconstructed using a newly developed computational code based on the Adaptive Neuro-Fuzzy Inference System (ANFIS) algorithm. Since ANFIS combines both neural network and fuzzy logic, it is capable of handling complex and non-linear problems. Unlike the situation in conventional neural networks, there is no vagueness in the ANFIS algorithm. The advantage of ANFIS with respect to classical neural networks is that prior knowledge given as fuzzy rules is able to be inserted within the network (rules such as: if temperature is hot then ...), thus providing a high probability of convergence toward a good generalization (the results with high accuracy).

## METHODS

### Algorithm and procedure for neutron energy spectrum unfolding

Neutron energy spectra,  $\varphi(E)$ , may be unfolded from the simulated/measured neutron pulse height distribution  $\frac{dN}{dH}$  obtained in the NE-213 liquid scintillator detector. How to simulate the neutron pulse height distribution is explained in the sections ‘Simulation of the neutron pulse height distribution’ and ‘Measurement of the neutron pulse height distribution’. The relation between the detector response matrix  $R(H, E)$ , the neutron pulse height distribution  $\frac{dN}{dH}$  and the neutron energy spectrum  $\varphi(E)$  is given by the Fredholm integral equation [11] as Eq. (1):

$$\frac{dN}{dH} = \int R(H, E) \varphi(E) dE \quad (1)$$

When the spectrum is recorded by a multichannel analyzer, Eq. (1) takes the discrete form as Eq. (2):

$$N_i = \sum_j R_{ij} \varphi_j \quad (2)$$

where  $N_i$  ( $i = 1, 2, \dots, n$ ) are the recorded counts on  $i$ th channel,  $\varphi_j$  ( $j = 1, 2, \dots, m$ ) is the energy spectrum in the  $j$ th energy interval, and  $R_{ij}$  is the response matrix coupling the  $i$ th pulse height interval with the  $j$ th energy interval. Eq. (2) may be transformed into matrix notation as in Eq. (3):

$$\bar{N} = \bar{R} \bar{\varphi} \quad (3)$$

where  $\bar{N} = (N_1, N_2, \dots, N_n)^T$ ,  $\bar{\varphi} = (\varphi_1, \varphi_2, \dots, \varphi_m)^T$ . Also,  $\bar{R}$  is the response matrix with size  $n \times m$ . Both Eqs (2) and (3) need to be inverted in order to obtain the neutron spectrum from the simulated neutron pulse height distribution ( $\bar{N}$ ), and it can be presented as a mapping from the simulated  $n$ -dimensional space of the detector response to the  $m$ -dimensional space of the neutron energy spectrum. The task of determining the unknown  $\bar{\varphi}$  from the observable  $\bar{N}$  presents an ill-conditioned problem. To unfold the spectrum, several mathematical methods and computing algorithms such as Monte Carlo [12], genetic algorithm [13] and artificial neural networks [3, 10] have been used. Unfolding of neutron energy spectra using artificial neural network has a relatively high calculation cost [10]. The main aim of the present work was development of a computational code based on a neuro-fuzzy algorithm in order to obtain highly accurate results with a low calculation cost. To this end, energy spectra of neutron sources were unfolded using a computational code based on the ANFIS algorithm, as described in the following.

An Adaptive Neuro-Fuzzy Inference System or adaptive network-based fuzzy inference system (ANFIS) is a kind of artificial neural network that is based on Takagi–Sugeno fuzzy inference system. The main concept in the ANFIS algorithm is eliminating some disadvantages of lonely-used of each fuzzy inference system and artificial neural network algorithms. The advantages of both mentioned algorithms are used to improve the effectiveness of the proposed algorithm in different applications such as modelling, control and classification [6–9]. ANFIS is considered to be a universal estimator for complex linear and non-linear systems [14]. The operation of ANFIS looks like that of a feed-forward back-propagation network. Output of the system is calculated forward, while premise parameters are calculated backward. Output variables are obtained by applying fuzzy rules to fuzzy sets of input variables. For example, the two rules associated with the structure in Fig. 1 will be as follows:

Rule 1: If  $x_1$  is  $A_{11}$  and  $x_2$  is  $A_{21}$  then  $f_1 = p_1 x_1 + q_1 x_2 + r_1$

Rule 2: If  $x_1$  is  $A_{12}$  and  $x_2$  is  $A_{22}$  then  $f_2 = p_2 x_1 + q_2 x_2 + r_2$

As shown in Fig. 1, ANFIS is structured into five layers:

#### Layer 1

Each node in this layer consists of a membership function  $A_i$ . The input for each node in this layer is  $x_i$  (one of system input), and the output is a number between 0 and 1 that shows the degree to which  $x_i$  satisfies  $A_k$ .  $A_i$  is a linguistic variable such as ‘small’, ‘big’, etc.

#### Layer 2

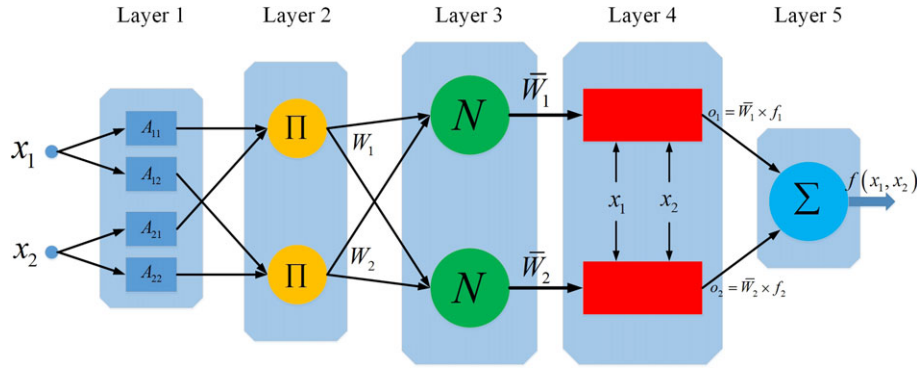


Fig. 1. The structure of ANFIS, consisting of five layers.

The output of nodes in this layer is the product of their inputs. For example  $W_1 = A_1(x_1) \times A_3(x_2)$ . Actually, the output of these nodes can be the application of any T-norm operator.

#### Layer 3

The output of the nodes in this layer is the ratio of the corresponding  $W_i$  (defined in Eq. (4)) to the sum of all  $W_k$ :  $k = 1: n$ .

$$\bar{W}_1 = \frac{W_1}{W_1 + W_2} \quad (4)$$

#### Layer 4

The output of the nodes in this layer are as determined by Eq. (5):

$$o_i = \bar{W}_i \times f_i = \bar{W}_i \times (p_i x_1 + q_i x_2 + r_i) \quad (5)$$

where  $\bar{W}_i$  is the output of the previous layer and  $\{p_i, q_i, r_i\}$  is the parameter set that is computed within the learning mechanism. There are two popular learning methods for ANFIS: the hybrid learning method and the back-propagation learning method.

#### Layer 5

The single node in this layer is used to compute the overall output of the system via Eq. (6):

$$f(x_1, x_2) = \sum_i o_i = \sum_i \bar{W}_i \times f_i \quad (6)$$

Computation of the parameters can be performed using various learning algorithms such as gradient descent or evolutionary. In the learning phase, parameters are selected so that the modeling error is minimized.

As shown in Fig. 1, ANFIS is used for modeling MISO (multiple-input single-output) systems. In the present problem, there is a MIMO (multiple-input multiple-output) system with 52 inputs and 52 outputs. Therefore, it is necessary to break the MIMO system into several simpler MISO systems. Each MISO system can be modeled with the ANFIS algorithm. The main steps are shown in Fig. 2.

### Simulation of the neutron pulse height distribution

As explained earlier, to reconstruct the energy spectrum of a neutron source, the neutron pulse height distribution in the detector should be known. Here, the neutron pulse height distributions of

4300 different energy spectra randomly generated by neutron sources (as detected by a NE-213 scintillator detector) were simulated using the developed MCNPX-ESUT computational code [5]. A database that included both simulated neutron pulse height distributions and corresponding randomly generated neutron energy spectra was generated.

To compare the simulated neutron pulse height distribution with the corresponding experimental data, the scintillation photon resolution function obtained from the experiment was considered in the simulation. The scintillation photon resolution  $\frac{\Delta L}{L}$  of the detector was parameterized [5, 15] in terms of the scintillation photon output  $L$  (in MeVee) as Eq. (7) [16]:

$$\frac{\Delta L}{L} = \sqrt{\alpha^2 + \frac{\beta^2}{L} + \frac{\gamma^2}{L^2}} \quad (7)$$

where the parameter  $\alpha$  is a dimensionless quantity, and  $\beta$  and  $\gamma$  have the units  $(\text{MeVee})^{0.5}$  and MeVee, respectively.

The presented scintillation photon resolution function in Eq. (7) includes various components, such as the locus-dependent scintillation photon transmission from the scintillator to the photocathode (first term), the statistical variation of the conversion of scintillation photons to photoelectrons (second term) and the noise contributions from the dynode chain (third term). The parameters  $\alpha$ ,  $\beta$  and  $\gamma$  in the present study were calculated by fitting a Gaussian function into the Compton edge of the considered known sources:  $^{137}\text{Cs}$ ,  $^{22}\text{Na}$  and  $^{60}\text{Co}$ . For each fitted Gaussian function, the related Full Width at Half Maximum (FWHM) was calculated. Fig. 3 shows the variations in the calculated  $\frac{\Delta L}{L}$  vs light. The calculated values for the light resolution parameters  $\alpha$ ,  $\beta$  and  $\gamma$ , through comparison of Fig. 3 and Eq. (7), are 0.1345, 0.1982 and 0.02, respectively. To validate the performed simulation using MCNPX-ESUT computational code, the neutron pulse height distributions due to  $^{252}\text{Cf}$  and  $^{241}\text{Am-}^9\text{Be}$  sources in an organic liquid scintillator NE-213 (5.08 cm, in height and 5.08 cm in diameter) were simulated.

### Measurement of the neutron pulse height distribution

The simulated neutron pulse height distribution should be validated against the experimental data. To measure the neutron pulse height

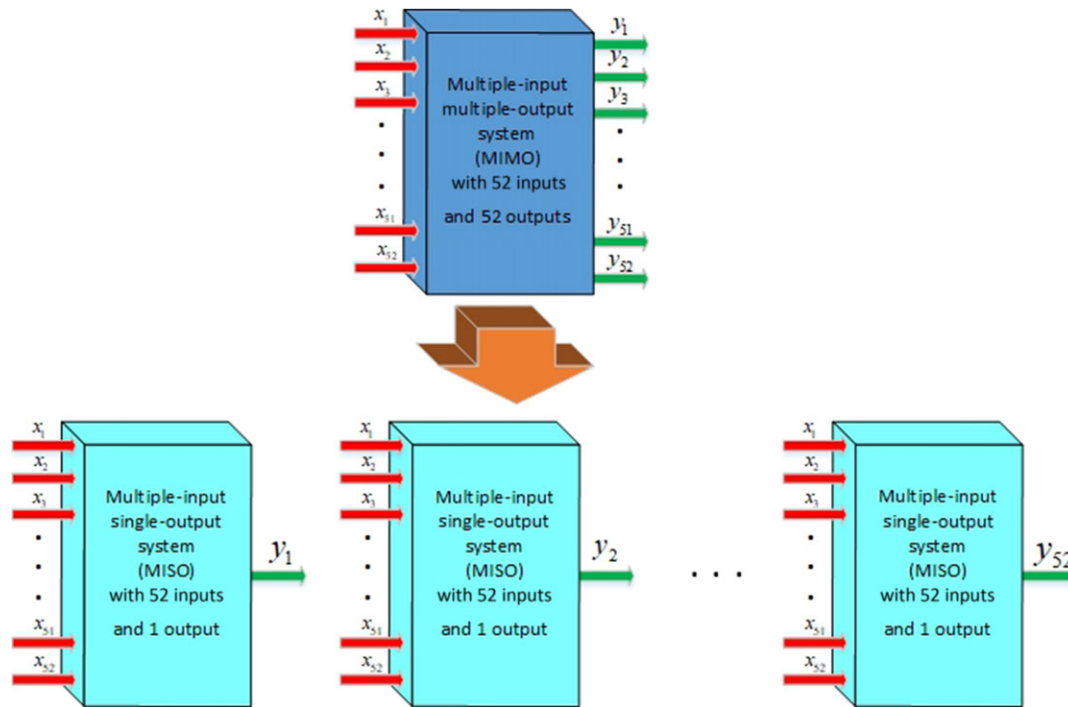


Fig. 2. Applying ANFIS requires breaking a MIMO system down into simpler MISO systems.

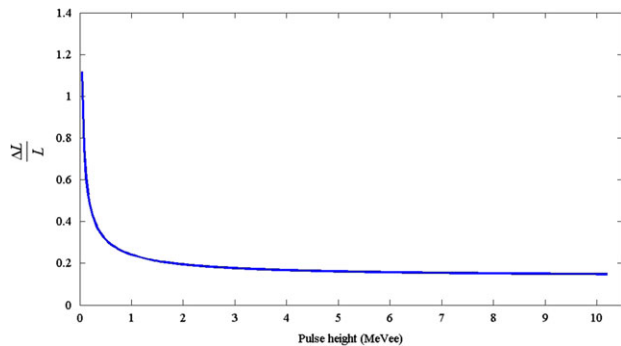


Fig. 3. Variation of detection resolution vs scintillation light output.

distribution in the mixed neutron and gamma fields, such as from the  $^{241}\text{Am-}^9\text{Be}$  source, neutron–gamma discrimination should be performed using an appropriate experimental set-up. Our detection system included a liquid scintillator container, a Photomultiplier Tube (PMT), a voltage divider and a magnetic shield. The containers were right cylinders made of aluminum of  $5.08 \times 5.08$  cm in size. Since the dynode chain structure affects the time needed for the electrons to reach the point at which the response signal is generated, the PMT choice has a critical effect on the energy and timing resolution, and is the key factor in pulse shape discrimination. To meet the research requirements, an Electron Tubes, 9814B type PMT (CFP company, Tehran, Iran) was selected. The 9814B is a 5.1 cm diameter, end-window photomultiplier with a blue-green sensitive bialkali photocathode and 12 BeCu dynodes of linear-focused design. To

cancel the effect of the Earth’s magnetic field on the PMT, a magnetic shield was used, as recommended by the manufacturer. Finally, the optical matching between the cell and the PMT was accomplished with silicon grease. In the present paper, the zero-crossing method [17] was used for neutron–gamma discrimination for the  $^{241}\text{Am-}^9\text{Be}$  source. The neutron pulse height distribution resulting from the  $^{241}\text{Am-}^9\text{Be}$  source was then obtained using the described neutron–gamma discrimination method. The neutron pulse height distribution from the  $^{252}\text{Cf}$  source was obtained using the same experimental set-up. These experiments were performed at the Radiation Detection Laboratory located in the Department of Energy Engineering at the Sharif University of Technology.

## RESULTS AND DISCUSSION

As explained earlier, the neutron pulse height distribution in the NE-213 detector was required in order to unfold the energy spectrum of the neutron source. Therefore, in the first stage of this research, the neutron pulse height distribution was obtained from the simulation performed using the MCNPX-ESUT computational code and the corresponding experimental method. Figs 4 and 5 show a comparison between the simulated and measured neutron pulse height distribution of  $^{252}\text{Cf}$  and  $^{241}\text{Am-}^9\text{Be}$  neutron sources, respectively. As shown, the simulated and measured neutron pulse height distributions have good agreement. Therefore, the simulated pulse height distribution may be used as input data in the unfolding procedure.

The motivation for the present study was the need for procedures that reconstruct the energy spectrum of a neutron source with high accuracy. Since the response matrix is usually close to singular or

badly scaled and its condition number is so high, unfolding of the neutron energy spectra via solution of the inverse problem by conventional algorithms leads to results with low accuracy. Therefore, in the present study, a computational code using a neuro fuzzy approach was developed, in which there is no need to solve the inverse problem. After validation of the simulated neutron pulse height distribution using MCNPX-ESUT computational code, it was used to generate the required input data for the training step in the ANFIS algorithm. To this end, the neutron pulse height distributions due to 4300 randomly generated energy spectra (the summation of the values energy spectrum in all bins is unit) were simulated. The simulated neutron pulse height distributions and corresponding neutron energy spectra were used as input and output data in the ANFIS unfolding algorithm. Figure 6 displays the unfolded energy spectrum of the  $^{241}\text{Am-}^9\text{Be}$  source as obtained using developed computational code based on the ANFIS algorithm approach. Also, the unfolded energy spectrum for  $^{252}\text{Cf}$  as obtained using the described method is presented in Fig. 7. As shown in Figs 6 and 7, there is excellent agreement between the unfolded energy spectra output using the ANFIS and ISO data [18]. Evidence for this claim is provided in Fig. 8, in which the difference between the neutron energy spectra (unfolded

and ISO) is presented. As shown, the size of the errors for calculations performed using ANFIS is much smaller than the errors reported in the previously published works [14, 19]. As displayed in Figs 6–8, the unfolded energy spectra of a neutron sources obtained using ANFIS are more accurate than the results obtained in the previously published paper by Hosseini [10]. The more accurate simulated neutron pulse height distributions lead to unfolding of the neutron

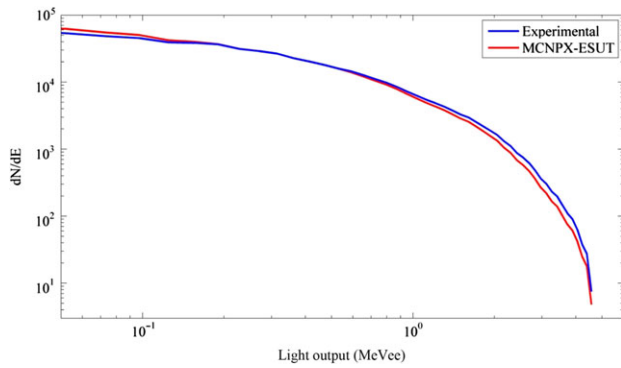


Fig. 4. Comparison of the simulated and measured neutron pulse height distributions from an  $^{241}\text{Am-}^9\text{Be}$  neutron source.

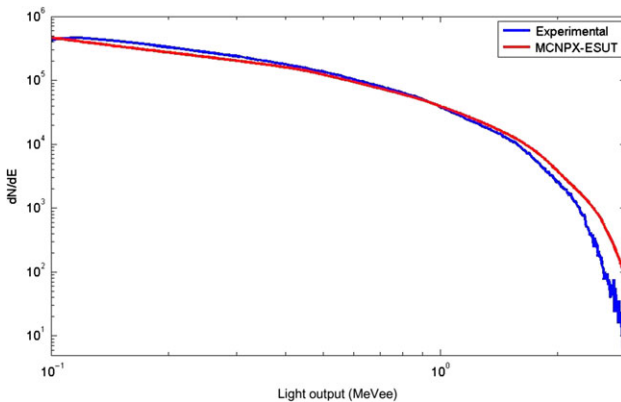


Fig. 5. Comparison of the simulated and measured neutron pulse height distributions from a  $^{252}\text{Cf}$  neutron source.

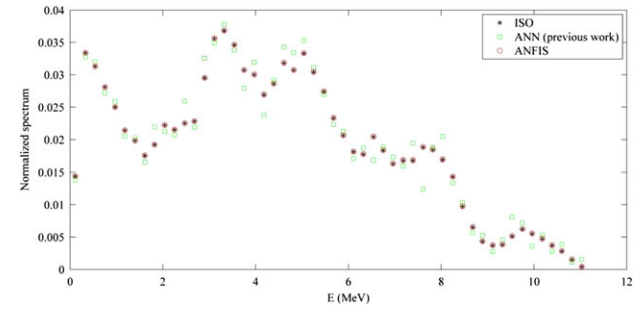


Fig. 6. Comparison of the unfolded neutron spectra of an  $^{241}\text{Am-}^9\text{Be}$  neutron source, the ISO data and the results reported in the previously published paper [10, 18].

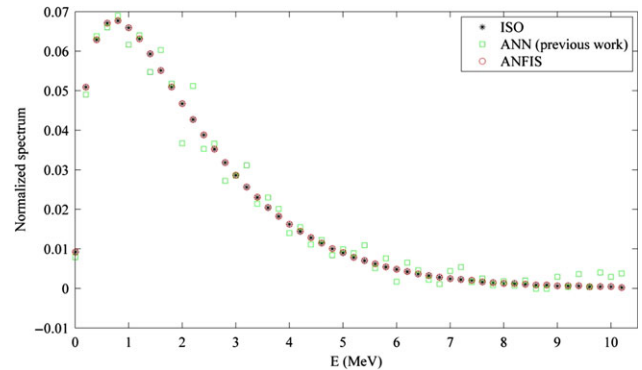


Fig. 7. Comparison of the unfolded neutron spectra of an  $^{252}\text{Cf}$  neutron source, the ISO results and the results reported in the previously published paper [10, 18].

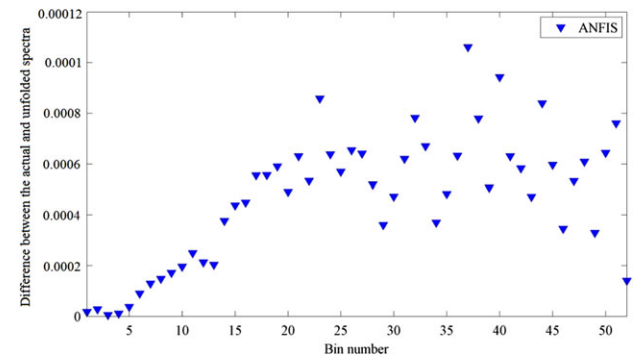


Fig. 8. Difference between the unfolded and actual neutron energy spectra.

energy spectra with greater accuracy. However, dependency of the accuracy of the unfolded neutron energy spectrum on the accuracy of the neutron pulse height distribution using the developed algorithm in the present work is less than when using iterative algorithms. From a computational cost point of view, it should be noted that the running time of the developed computer code based on the ANFIS algorithm for 4300 spectra is close to 1 min, whereas the same calculation using an artificial neural network based on logsig and tansig transfer functions takes 45 min.

### CONCLUSION

In this study, the energy spectra of neutron sources was reconstructed using the developed computational code based on the ANFIS algorithm. The developed MCNPX-ESUT computational code was used to simulate the neutron pulse height distribution in an NE-213 scintillator detector. Comparison between the reconstructed energy spectra and reference data for  $^{252}\text{Cf}$  and  $^{241}\text{Am}$ - $^9\text{Be}$  confirms the correctness of the calculation. The results obtained from the developed computational code based on the ANFIS method have excellent agreement with the reference data. Accurate knowledge of neutron energy spectra is of great importance in much basic research and in many applications such as in nuclear non-proliferation, international safeguarding, nuclear material control, national security and counterterrorism. We conclude that the developed computational code based on the ANFIS algorithm may be considered to be a reliable tool for unfolding the energy spectra of neutron sources.

### FUNDING

The first author is grateful to the research office of the Sharif University of Technology for the support of the present work.

### REFERENCES

1. Flaska M, Pozzi S. Pulse-shape discrimination for identification of neutron sources using the BC-501A liquid scintillator. In: *Proceedings of the 8th Joint International Topical Meeting on Mathematics & Computation and Supercomputing in Nuclear Applications (M&C+ SNA 2007)*, 2007, 15–19.
2. Mullens JA, Edwards JD, Pozzi SA. Analysis of scintillator pulse-height for nuclear material identification. In: *Institute of Nuclear Materials Management 45th Annual Meeting, Orlando, FL*, 2004.
3. Avdic S, Pozzi SA, Protopopescu V. Detector response unfolding using artificial neural networks. *Nucl Instrum Methods Phys Res A* 2006;565:742–52.
4. Marrone S, Cano-Ott D, Colonna N et al. Pulse shape analysis of liquid scintillators for neutron studies. *Nucl Instrum Methods Phys Res A* 2002;490:299–307.
5. Hosseini SA, Vosoughi N, Zangian M. Development of MCNPX-ESUT computer code for simulation of neutron/gamma pulse height distribution. *Nucl Instrum Methods Phys Res A* 2015;782:112–9.
6. Reginatto M, Goldhagen P, Neumann S. Spectrum unfolding, sensitivity analysis and propagation of uncertainties with the maximum entropy deconvolution code MAXED. *Nucl Instrum Methods Phys Res A* 2002;476:242–6.
7. Matzke M. Unfolding of particle spectra. In: *Fifth International Conference on Applications of Nuclear Techniques: Neutrons in Research and Industry. International Society for Optics and Photonics*, 1997, 598–607.
8. Matzke M. *Unfolding of Pulse Height Spectra: the HEPRO Program System*. Wirtschaftsverl NW: Neue Wiss, 1994.
9. Johnson RH, Wehring BW. The FORIST unfolding code. ORNL/RSIC Newsletter No. 40 1976, 33.
10. Hosseini SA. Neutron spectrum unfolding using artificial neural network and modified least square method. *Radiat Phys Chem* 2016;126:75–84.
11. Knoll GF. *Radiation Detection and Measurement*. Ann Arbor, Michigan: John Wiley & Sons, 2010.
12. Sanna R, O'brien K. Monte-Carlo unfolding of neutron spectra. *Nucl Instrum Methods* 1971;91:573–6.
13. Mukherjee B. BONDI-97: a novel neutron energy spectrum unfolding tool using a genetic algorithm. *Nucl Instrum Methods Phys Res A* 1999;432:305–12.
14. Ido AS, Bonyadi M, Etaati G et al. Unfolding the neutron spectrum of a NE213 scintillator using artificial neural networks. *Appl Radiat Isot* 2009;67:1912–8.
15. Dietze G, Klein H. Gamma-calibration of NE 213 scintillation counters. *Nucl Instrum Methods Phys Res* 1982;193:549–56.
16. Dekempeneer E, Liskien H, Mewissen L et al. A spectrometer for double-differential neutron-emission cross section measurements in the energy range 1.6 to 16 MeV. *Nucl Instrum Methods Phys Res A* 1987;256:489–98.
17. Nakhostin M, Walker P. Application of digital zero-crossing technique for neutron-gamma discrimination in liquid organic scintillation detectors. *Nucl Instrum Methods Phys Res A* 2010; 621, 498–501.
18. Park S-T. Neutron energy spectra of  $^{252}\text{Cf}$ , Am-Be source and of the D (d, n)  $^3\text{He}$  reaction. *J Radioanal Nucl Chem* 2003;256: 163–6.
19. Chen Y, Chen X, Lei J et al. Unfolding the fast neutron spectra of a BC501A liquid scintillation detector using GRAVEL method. *Sci China Phys Mech Astron* 2014;57:1885–90.